Biochimica et Biophysica Acta, 942 (1988) 305–314
Elsevier

BBA 74070

Structural rearrangements during crystal–liquid-crystal and gel–liquid-crystal phase transitions in aqueous dispersions of dipalmitoylphosphatidylethanolamine. A time-resolved X-ray diffraction study

Boris G. Tenchov *, Leonard J. Lis ** and Peter J. Quinn

Department of Biochemistry, King's College London, London (U.K.)

(Received 18 January 1988)

Key words: Phosphatidylethanolamine; Phase transition; X-ray diffraction; Time resolved X-ray diffraction

The mechanism and kinetics of the crystal–liquid-crystal ($L_c \rightarrow L_\alpha$) and gel–liquid-crystal ($L_\beta \leftrightarrow L_\alpha$) transitions of the L-enantiomer and racemic dipalmitoylphosphatidylethanolamine have been examined in temperature scans and jumps using time-resolved X-ray diffraction methods. The $L_c \rightarrow L_\alpha$ transformations (at 66 °C for L-dipalmitoylphosphatidylethanolamine and 82 °C for DL-dipalmitoylphosphatidylethanolamine) were found to be two-state (first-order) processes characterised by co-existence of the initial L_c and final L_α states during the transition with the absence of any detectable intermediates states. The transition mechanism involves firstly, disordering of the hydrocarbon chains which makes a major contribution to the transition enthalpy and secondly by a transition in the lamellar repeat spacing. The overall relaxation time of the $L_c \rightarrow L_\alpha$ transition of L-dipalmitoylphosphatidylethanolamine during temperature jumps of 4.5 C°/s was about 10 s. A gradual increase in the gel-state interchain spacing during the $L_\beta \leftrightarrow L_\alpha$ transitions of L- and DL-dipalmitoylphosphatidylethanolamine preceeded a broadening of the wide-angle diffraction peak. There was a concomitant and continuous increase of the lamellar repeat spacing to values typical of the L_α phase with increasing temperature. This sequence of events is completely reversible on cooling with a temperature hysteresis of 5–6 C°. The relaxation times of the $L_\beta \leftrightarrow L_\alpha$ transitions during jumps of 4.5 C°/s were about 2 s in both the heating and cooling directions.

Introduction

Phosphatidylethanolamines constitute one of the major phospholipid classes in biological membranes. When dispersed in water or dilute salt solutions they display rich polymorphism depending on water content, temperature, thermal prehistory and the presence of various electrolytes. The saturated diacyl and dialkyl phosphatidylethanolamines in excess water, for example, have been shown to form at least four different phases, namely, a crystalline lamellar phase (L_c) and a metastable lamellar gel phase (L_β) at low temperatures, a lamellar liquid-crystalline phase (L_α) at intermediate temperatures and an inverted hexagonal phase (H_{II}) at elevated temperatures [1–7]. In addition, Seddon et al. [4] have shown that dilaurylphosphatidylethanolamine can form two different L_c phases; an equilibrium phase with the acyl chains perpendicular to the bilayer surface

* Present address: Central Laboratory of Biophysics, Bulgarian Academy of Sciences, 1113 Sofia, Bulgaria.
** Present address: Department of Physics and Liquid Crystal Institute, Kent State University, Kent, OH, 44242, U.S.A.

Correspondence: P.J. Quinn, Department of Biochemistry, King's College London, Campden Hill, London W8 7AH, U.K.

(designated β_1) and a metastable phase with tilted chains (designated β_2).

The structures of all these phases have been relatively well characterised by static X-ray diffraction studies. The precise mechanisms and order of the phase transformations between the different phases, however, are presently not well understood. One method of approaching this problem is to exploit recent developments in time-resolved X-ray diffraction methods that employ intense radiation from synchrotron sources. The photon flux from these sources is sufficiently high as to enable diffraction patterns to be recorded during time intervals necessary to provide information on the sequence and kinetics of the structural events that take place with changing temperature during the phase transitions in lipid membranes. These methods have already been successfully employed for studies of various lipid phase transitions including the lamellar-gel to liquid-crystal transitions [8,9], the pretransition [9] and the subtransition [10] of saturated phosphatidylcholines in aqueous dispersions. Transitions between lamellar gel, lamellar liquid-crystal and lamellar and non-lamellar phases of dihexadecylphosphatidylethanolamine [11] and egg phosphatidylethanolamine [9] in aqueous systems have also been reported. Lipid phase transitions in non-aqueous media [12] and fusion of lamellar and H_{II} phases [13] are other systems that have been investigated by time-resolved synchrotron X-ray diffraction methods.

In the present work we have applied time-resolved X-ray diffraction to examine the structural changes associated with the crystal–liquid crystal ($L_c \rightarrow L_\alpha$) and gel–liquid-crystal ($L_\beta \leftrightarrow L_\alpha$) transitions of L- and DL-dipalmitoylphosphatidylethanolamine dispersed in excess water. The formation of different structures by the L- and the DL-dipalmitoylphosphatidylethanolamines is strongly implied in a recent differential scanning calorimetric study [14]. A similar situation exists in the phosphatidylcholines where Sakurai et al. [25] showed that the L- and the DL-modifications pack into different crystal structures at low levels of hydration. Moreover, the formation of the L_c phase in fully hydrated racemic dipalmitoylphosphatidylcholine has been shown to be hindered [15].

The X-ray data reported here shows that the $L_c \rightarrow L_\alpha$ transition of dipalmitoylphosphatidylethanolamine proceeds as a two-state process and that it is considerably slower than the $L_\beta \leftrightarrow L_\alpha$ transition. The latter transition, however, appears to proceed by a non first-order (two-state) thermodynamic process.

Materials and Methods

L-Dipalmitoylphosphatidylethanolamine and DL-dipalmitoylphosphatidylethanolamine were obtained from Fluka AG and used without further purification. Analysis by thin layer and gas chromatography showed both lipids to be greater than 99% pure [14].

The phospholipids were dissolved in chloroform/methanol (9 : 1, v/v), the solvent removed by rotary evaporation under nitrogen and the lipid dried for 6 h under vacuum. The lipids were hydrated with sodium borate buffer (50 mM, pH 8.0) to give a lipid concentration of 10 wt%. The lipid was removed from the glass walls by brief sonication (30 s), hydrated overnight at 20 °C and sonicated again for 30 s. The dispersion was subjected to centrifugation at $100\,000 \times g$ for 5 min and the pellet equilibrated for at least 4 days prior to X-ray examination. The final lipid concentration was 25–30 wt%, dipalmitoylphosphatidylethanolamine/buffer. All procedures were performed at about 20 °C.

Differential scanning calorimetry of dilute lipid dispersions (0.003 wt%) was performed using a Privalov differential adiabatic scanning calorimeter (DASM-1M) at a heating rate of 0.5 C°/min. X-ray experiments were carried out using a monochromatic (0.150 nm) focussed X-ray beam at station 7.2 of the Daresbury Synchrotron Laboratory as previously described [16]. A cylindrically bent single crystal of Ge [17] and a long float glass mirror were used to select monochromatic X-rays and to focus the beam horizontally to provide about $2 \cdot 10^9$ photons/s through a 0.2 mm colimator at 2.0 GeV and 100 to 200 mA of electron beam current. A Keele flat plate camera was used with a linear wire detector constructed at Daresbury. The detector contained 515 channels each of 0.193 mm. The counting efficiency was approximately 60% at a total count rate of 10^6 cps. The

detector response was determined by recording a signal from a fixed source accumulated over several hours; the data was stored in a VAX-11/750 computer and used to correct experimental data sets for detector response. The raw scattering data were subjected to a smoothing routine using cubic splines. X-ray scattering data was acquired in 255 consecutive time frames with a dead time between each frame of 50 μs. The acquisition time of each frame was 150 ms for the temperature jump experiments and 1.2 or 3.5 s for temperature scans. X-ray scattering was plotted as a function of reciprocal spacings using teflon as a calibration standard [18].

Temperature scans and jumps were produced by water baths connected internally to the sample mount of the X-ray camera; the maximum rate of change of temperature was about 4 C°/s. The temperature of the sample was monitored internally using a thermocouple placed adjacent to the sample in the X-ray sample holder.

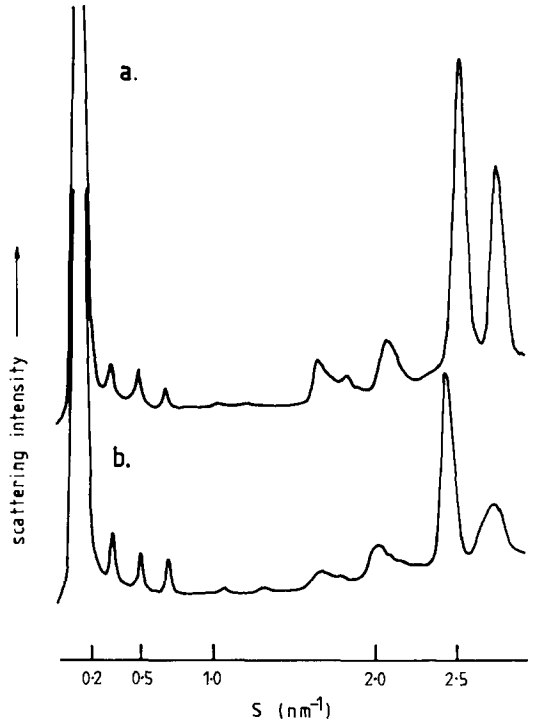

Fig. 1. Diffraction patterns of (a) L-dipalmitoylphosphatidylethanolamine and (b) DL-dipalmitoylphosphatidylethanolamine in the crystalline L_c phase recorded at 20 °C with a accumulation time of 100 s.

Results

The major difference in the thermal behaviour of L- and DL-dipalmitoylphosphatidylethanolamine dispersed in excess water is that the $L_c \rightarrow L_\alpha$ transition of L-dipalmitoylphosphatidylethanolamine occurs at 65–66 °C [6] while the corresponding transition of DL-dipalmitoylphosphatidylethanolamine takes place at 82 °C [14]. After equilibration in the L_α phase, cooling of the samples transforms them both into a lamellar gel phase (L_β) and a second heating scan performed immediately after the cooling stage produces in both cases the well-known $L_\beta \rightarrow L_\alpha$ transitions at 63–64 °C.

Static diffraction patterns of the L_c phase recorded at 20 °C provide evidence for a slightly different arrangement of the lipid molecules in the

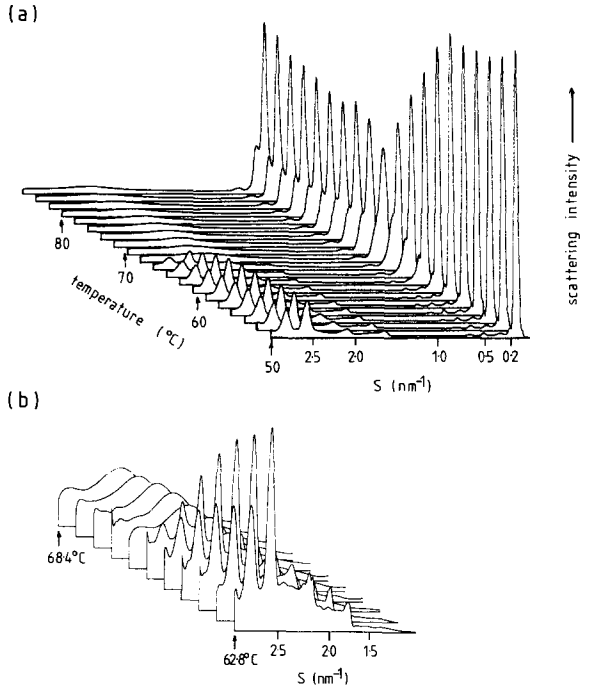

Fig. 2. Three-dimensional plot of X-ray scattering intensity versus reciprocal spacing during a scan from 50 to 80 °C at 10 C°/ min through the $L_c \rightarrow L_\alpha$ transition of L-dipalmitoylphosphatidylethanolamine dispersed in excess water. Every third frame of the complete data set recorded is plotted. Accumulation time of the individual diffraction patterns was 3.5 s. (b) Three-dimensional plot of the wide-angle region during the transition. The set consists of eleven successive diffraction patterns recorded over the temperature range indicated.

unit cells of L- and DL-dipalmitoylphosphatidylethanolamine (Fig. 1). It can be seen that the lamellar repeat distances are identical in the two lipids (5.7 nm) at this temperature. The wide-angle scattering patterns are typical 'powder' patterns of the lipid subgel phases with two intense scattering peaks and at least two weaker intensity bands at longer spacings. The spacings of these four bands are 0.360, 0.390, 0.470 and 0.582 nm for L-dipalmitoylphosphatidylethanolamine and 0.370, 0.403, 0.475 and 0.584 nm for DL-dipalmitoylphosphatidylethanolamine. Similar 'powder' wide-angle X-ray patterns have been obtained for the equilibrium L_c phase (denoted β_2) of dilauroylphosphatidylethanolamine [4] and indexed on an orthorhombic lattice although the actual lattice is rather monoclinic or triclinic but with all angles close to 90°. Such indexing on a similar orthorhombic hybrid subcell produces subcell dimensions of $a_s = 0.943$ nm and $b_s = 0.750$ nm for L-dipalmitoylphosphatidylethanolamine, and $a_s = 0.986$ nm and $b_s = 0.770$ nm for DL-dipalmitoylphosphatidylethanolamine. The long axis for the unit cell is 5.7 nm in both lipids while the subcell c_s axis is 0.254 nm for all hydrocarbon chain modes. The two-dimensional areas per molecule are thus calculated to be 0.354 nm^2 and 0.380 nm^2 (giving areas of acyl chains of 0.177 and 0.190 nm^2) for the L- and DL-dipalmitoylphosphatidylethanolamines, respectively. The cross-sectional area of L-dipalmitoylphosphatidylethanolamine is approximately the same as that calculated for L-dilaurylphosphatidylethanolamine from the data of Seddon et al. [19] and the cross-sectional areas of both phosphatidylethanolamines are less than L-dipalmitoylphosphatidylcholine (0.397 nm^2) [10] when all are in similar phase states.

The observed difference in the acyl chain subcell spacings of L- and DL-dipalmitoylphosphatidylethanolamine suggests that, although the lamellar repeat is not dependent on the particular enantiomer, the lateral interactions in the bilayer

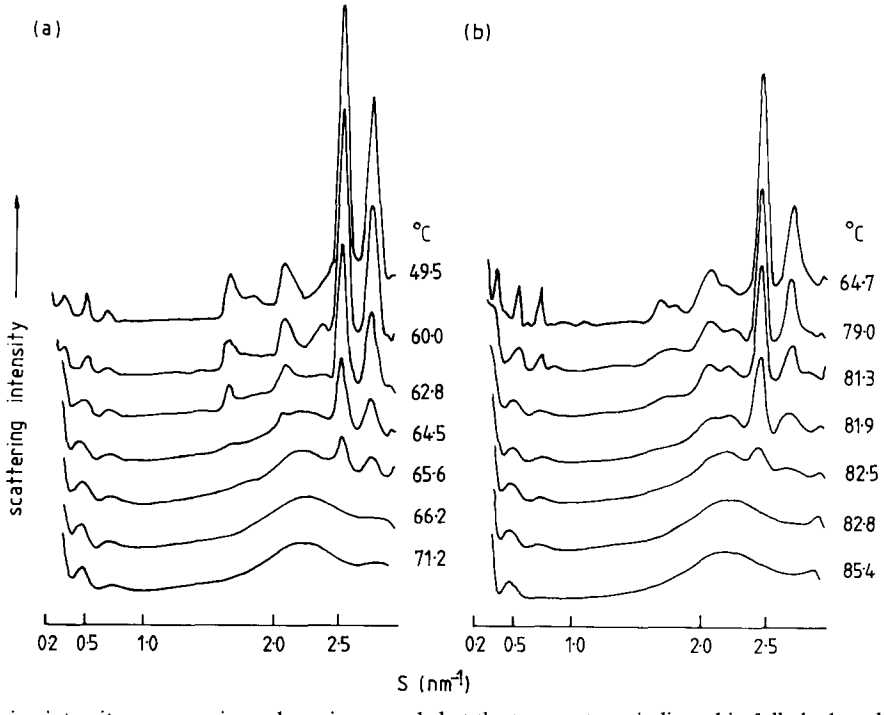

Fig. 3. X-ray scattering intensity versus reciprocal spacing recorded at the temperatures indicated in fully hydrated dispersions of (a) L-dipalmitoylphosphatidylethanolamine and (b) DL-dipalmitoylphosphatidylethanolamine equilibrated in the L_c phase and heated through the $L_c \rightarrow L_\alpha$ phase transition at 10 C°/min. Each diffraction pattern was accumulated in 3.5 s.

are influenced with a resulting closer packing of the acyl chains in the unit cell of L-dipalmitoylphosphatidylethanolamine.

Crystal-liquid crystal transitions

The $L_c \rightarrow L_\alpha$ transitions are observed by calorimetry during the first heating scans of samples equilibrated at low temperature. An overview of the corresponding structural changes recorded by X-ray diffraction measurements during the $L_c \rightarrow L_\alpha$ transition in L-dipalmitoylphosphatidylethanolamine is presented in Fig. 2. This shows a three-dimensional plot of the diffraction intensity versus reciprocal spacing recorded at intervals of 3.5 s during a temperature scan of 10C°/min through the transition. The phase transition is clearly distinguished in both the low- and wide-angle regions of the diffraction patterns. The changes in the wide-angle scattering, shown in greater detail in the inset to Fig. 2, indicate a progressive decrease in intensity of the peaks indexed to the ordered acyl chain packing in the L_c phase and the gradual appearance of a broad scattering band characteristic of the liquid-crystalline phase. The precise mechanism of disappearance of the L_c and appearance of the L_α phase in L- and DL-dipalmitoylphosphatidylethanolamine is shown in Fig. 3. The peaks characteristic of the L_c phase are seen to decrease monotonically in intensity until they finally disappear. There is no apparent broadening or shift in the spacing of these bands during the transition. Concomitantly, there is an increase in intensity of the broad scattering band centred at 0.45 nm which typifies the L_α phase. There is no evidence of any structural intermediates between the crystalline and liquid crystalline phases. This behaviour is observed both in L- and DL-dipalmitoylphosphatidylethanolamines and indicates identical two-state pathways for the $L_c \rightarrow L_\alpha$ phase transition.

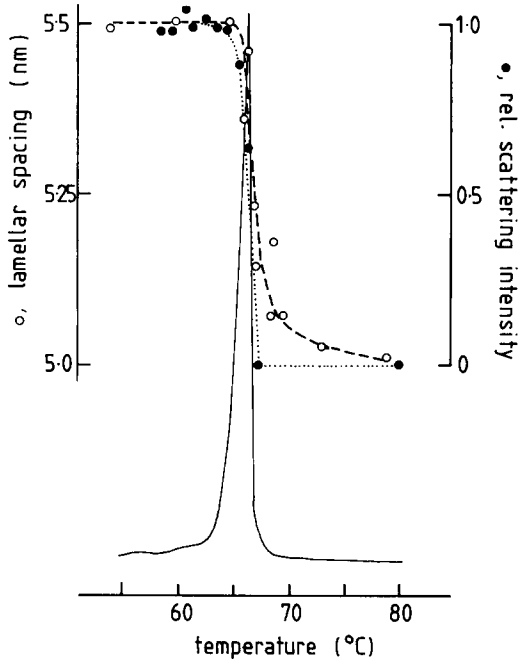

Fig. 4. The relationship between calorimetric and X-ray diffraction data recorded during the $L_c \rightarrow L_\alpha$ phase transition of L-dipalmitoylphosphatidylethanolamine in excess water. ———, excess heat capacity; (· · · · · ·), X-ray scattering intensity of the wide-angle diffraction pattern of the L_c phase; (— — —), lamellar period.

Apart from changes in hydrocarbon chain spacing, the $L_c \rightarrow L_\alpha$ transition of L-dipalmitoylphosphatidylethanolamine is also accompanied by a decrease in the lamellar repeat spacing from about 5.5 nm to 5.0 nm in the transition region (Fig. 4). The data shown in Fig. 3 also indicates that the only difference in the $L_c \rightarrow L_\alpha$ transitions of L- and DL-dipalmitoylphosphatidylethanolamine are the different temperatures at which these transitions take place.

The kinetics of the $L_c \rightarrow L_\alpha$ transition in aqueous dispersions of L-dipalmitoylphosphatidylethanolamine were investigated in temperature jump experiments. Representative diffraction patterns recorded with an acquisition time of 150 ms are presented in a three-dimensional plot in Fig. 5. As a consequence of the short accumulation time the individual diffraction patterns on this time-scale show considerable fluctuations in position and shape of the diffraction peaks. As noted previously [10] addition of the scattering intensities from successive diffraction patterns recorded over 1 second duration usually averages out these fluctuations and produces stable and smooth profiles. Fig. 5b shows a plot of scattering intensities accumulated over 10 successive 150 ms data frames. It can be seen that fluctuations observed on the 150 ms time scale are eliminated.

Examination of the time-resolved data in Fig. 5 and similar data for DL-dipalmitoylphosphatidyl-

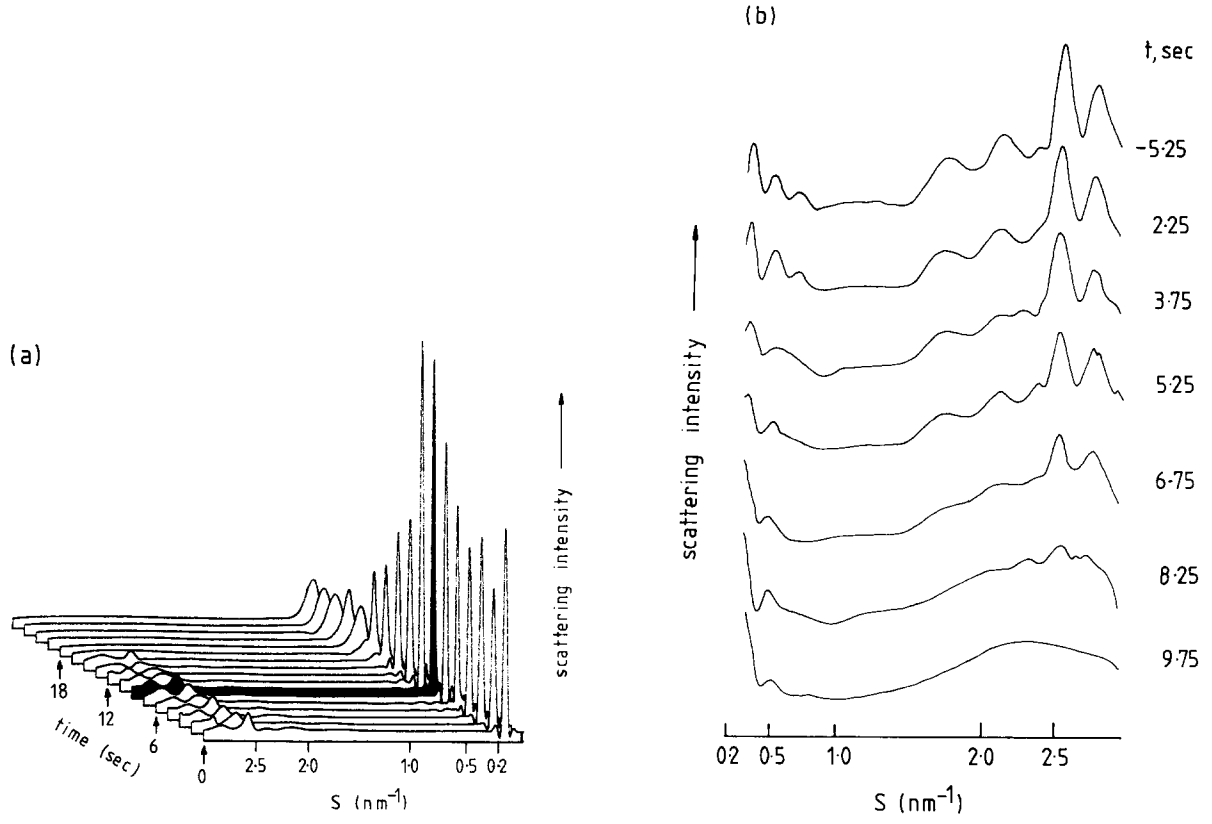

Fig. 5. X-ray scattering intensity versus reciprocal spacing recorded from 25 to 75 °C for the $L_c \rightarrow L_\alpha$ transition of L-dipalmitoylphosphatidylethanolamine driven by a temperature jump of 4.5 C°/s. (a) Three-dimensional plot of diffraction patterns accumulated over 150 ms. Every 10th frame is shown. The diffraction pattern recorded at the transition temperature is shaded; (b) diffraction patterns accumulated over 1.5 s. The time from when the transition temperature was reached is indicated.

ethanolamine (not shown) indicates that the wide-angle patterns characteristic of the L_c phase, although decreasing in intensity, persist for about 9 s after the temperature recorded by the thermocouple exceeds the transition temperature of 66 °C, finally giving way to the liquid-crystalline phase. Concomitantly with the decrease of diffraction intensity arising from the chain packing of the L_c phase, the second and higher-order low-angle lamellar reflections broaden and disappear. However, the first-order reflection retains its position at 5.5 nm during the whole 9 s period where the L_c phase is still present, according to the wide-angle diffraction, and shifts to the value 5.0 nm typical of the L_α phase during the first second after complete disappearance of the L_c phase in the wide-angle region. These observations indicate that the overall transit time of the $L_c \rightarrow L_\alpha$ transformation is about 10 s in our experimental conditions in which the wide-angle reflections of the L_c phase disappears 9 s after the temperature passes the phase transition temperature of 66 °C and this is followed by a 1 s transition of the lamellar period. It is also noteworthy that the intensity profile for the low-angle reflections in Fig. 5a is different from that of the final L_α structure observed during the temperature scans shown in Fig. 2. The small-angle reflections at the end of the temperature jump are characteristic of the region of instability between the L_β and L_α equilibrium phase states. It is clear that the formation of the final L_α ordered array requires a longer time than recorded during the temperature jump experiment.

Gel–liquid-crystal transition

The gel–liquid-crystal phase transition was investigated by cooling and subsequently heating samples equilibrated in the L_α phase. Examples of

$L_\beta \rightarrow L_\alpha$ and $L_\alpha \rightarrow L_\beta$ transformations are shown in Figs. 6a and 6b. These sequences of diffraction patterns are completely reversible with a temperature hysteresis of 5–6 C° (Fig. 8). The process of the $L_\beta \rightarrow L_\alpha$ conversion in the wide-angle scattering region is illustrated in greater detail in Fig. 7. A slow increase of the gel-phase interchain distance with increasing temperature is replaced in the transition region by broadening of the wide-angle peak and an increase of its spacing to values typical of the liquid crystal phase (Fig. 8). There is evidence also for co-existence of the two phases

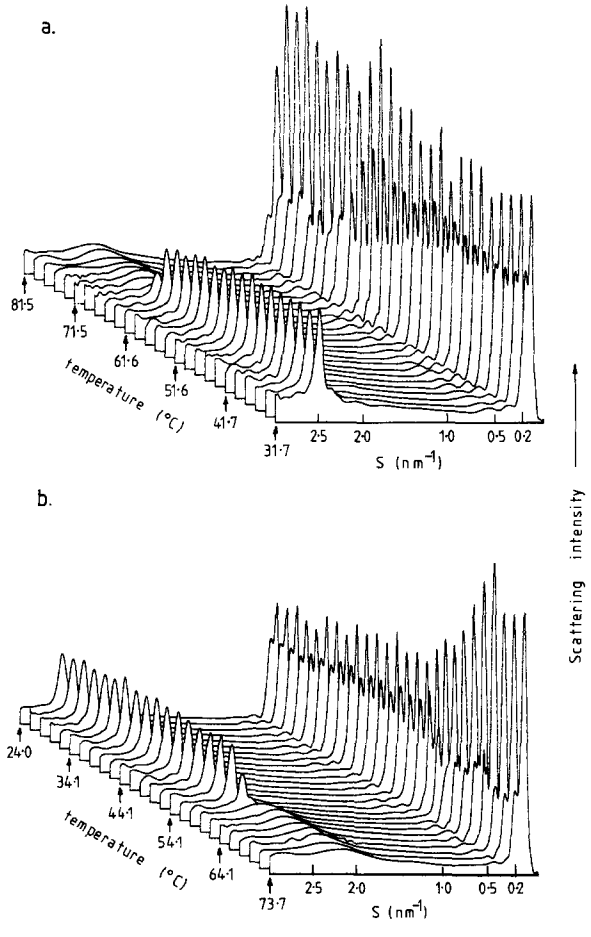

Fig. 6. Three-dimensional plots of X-ray scattering intensity versus reciprocal spacing of hydrated L-dipalmitoylphosphatidylethanolamine during (a) heating and (b) cooling scans at 10 C°/min through the $L_\beta \rightarrow L_\alpha$ phase transition. Diffraction patterns were accumulated during 1.2 s; only every 10th frame of the complete data set is shown. The sequence illustrated is also representative of the $L_\beta \leftrightarrow L_\alpha$ phase transitions observed in hydrated DL-dipalmitoylphosphatidylethanolamine.

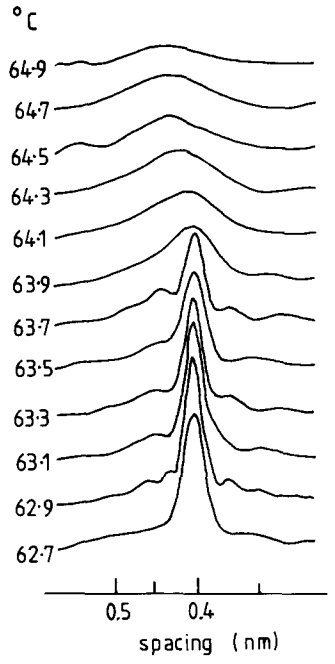

Fig. 7. Successive wide-angle X-ray diffraction patterns recorded during 1.2 s showing the process of the $L_\beta \rightarrow L_\alpha$ transformation of hydrated L-dipalmitoylphosphatidylethanolamine during heating at 10 C°/min. The temperature at which each observation was made is indicated. The sequence is completely reversible on cooling with a temperature hysteresis of 5–6 C° (see Fig. 8). The changes are also representative of the $L_\beta \rightarrow L_\alpha$ transition in hydrated DL-dipalmitoylphosphatidylethanolamine.

but only in individual diffraction patterns and not consistently throughout the whole transition region. Nevertheless, it is not possible to represent the broad symmetric bands centered at intermediate positions as a superposition of the sharp diffraction peaks characteristic of L_β and the diffuse band typical of L_α phase. The accompanying change of the lamellar period takes place simultaneously with the transition observed in wide-angle scattering region (Fig. 8). Compared to the two-state $L_c \rightarrow L_\alpha$ transition, this sequence of structural events suggests a somewhat different transition mechanism involving detectable intermediate states.

The kinetics of the $L_\beta \rightarrow L_\alpha$ and $L_\alpha \rightarrow L_\beta$ transformantions were investigated by temperature jumps of 4.5 C°/s in the same manner as described above for the $L_c \rightarrow L_\alpha$ transition. In the cooling direction, the L_α phase was observed for 1

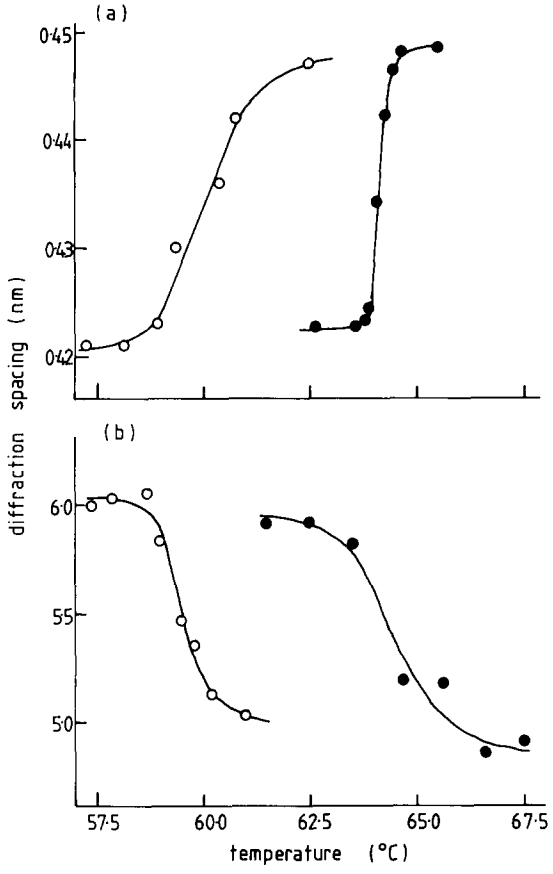

Fig. 8. Temperature dependence of the spacing corresponding to the wide-angle scattering maxima of hydrated L-dipalmitoylphosphatidylethanolamine during the $L_\beta \leftrightarrow L_\alpha$ transition in (●) heating and (○) cooling scans at 10 C°/min.

sec after the temperature decreased below 60 °C (down to about 55 °C) and after which it was transformed to L_β phase over a period of about 1 s. Thus, the overall transit time was about 2 s. In the heating direction the transit time was also found to be about 2 s. The $L_\beta \leftrightarrow L_\alpha$ transformations of the L- and DL-dipalmitoylphosphatidylethanolamine appeared to proceed in an identical manner.

Discussion

Racemic substances can exist in three principally different states depending on the relative strength of the interaction between antipode and similar enantiomers [20]. Racemic mixtures and solutions, on the one hand, and racemic compounds on the other, are characterised by different, easily discernible phase diagrams. It has been suggested that the greater thermal stability of the L_c phase of DL-dipalmitoylphosphatidylethanolamine compared with the L_c phase of the pure L-enantiomer is due to the formation of a racemic compound at low hydration in which there is a stronger attraction in the DL pairs than in the LL and DD pairs [14]. These intermolecular complexes appear to dissociate after equilibration in the L_α phase and, in the hydrated state, the racemic dipalmitoylphosphatidylethanolamine forms a nearly ideal solution which is characterised by an $L_\beta \leftrightarrow L_\alpha$ transition very similar in character and temperature to that of L-dipalmitoylphosphatidylethanolamine.

Our wide-angle data suggest that the greater thermal stability of DL-dipalmitoylphosphatidylethanolamine in the L_c phase is not associated with a closer packing of the acyl chains in the unit cell; it could be due to additional interactions at the bilayer surface. The hydrogen bond network in the polar group region of bilayers of phosphatidylethanolamine [21] is likely to play an important role in this respect. To account for the greater thermal stability of the L_c phase of DL-dipalmitoylphosphatidylethanolamine, it could be argued that the mutual orientation of DL pairs is more conducive to intermolecular hydrogen bonding than in LL and DD pairs despite the denser packing arrangement in the pure enantiomer.

Time-resolved X-ray data presented here provide indications that the $L_c \rightarrow L_\alpha$ and $L_\beta \leftrightarrow L_\alpha$ phase transitions proceeed by different mechanisms. Thus the $L_c \rightarrow L_\alpha$ transitions of the L- and DL-dipalmitoylphosphatidylethanolamine appear to be two-state processes characterised by co-existence of the initial L_c and final L_α states with the absence of any detectable intermediate states. During this transition, the wide-angle diffraction pattern of the L_c phase decreased in intensity without any shift in position or broadening of the peaks while the wide-angle band of the L_α phase appeared at a diffraction spacing corresponding to 0.45 nm and increased in intensity without change in spacing. The absence of detectable intermediate states leads to the conclusion that, at least at the time resolution of our experiments (1.2 and 3.5 s

in the temperature scans and 150 ms in the temperature jumps), the $L_c \rightarrow L_\alpha$ transitions of the L- and DL-dipalmitoylphosphatidylethanolamine are two-state (first-order) phase transitions.

During the $L_\beta \rightarrow L_\alpha$ transition of dipalmitoylphosphatidylethanolamine the gel-phase wide-angle band appears to broaden first and then shift to spacings characteristic of the L_α phase (Figs. 7 and 8). This process cannot be characterised either as a pure two-phase co-existence or as a monotonically continuous process exemplified by the subtransition of L-dipalmitoylphosphatidylcholine [10]. Instead, the process appears to combine features of both a two-state and a continuous phase transition. Some confidence in such an 'intermediate order' interpretation is provided by studies of gel–liquid-crystalline phase transitions by alternating-current calorimetry reported by Hatta et al. [22,23] who concluded that the $P_{\beta'}$ to L_α phase transition of fully hydrated dipalmitoylphosphatidylcholine is a 'weak first-order' transition combining true enthalpy absorption with a specific heat anomaly. However, compared with calorimetric studies our data were obtained at relatively high heating rates (10 °C/min) and this may introduce some, as yet unrecognised, kinetic factors. It is obvious that a more direct correspondence would probably emerge if time-resolved X-ray data were recorded during quasistatic heating of the sample. In this connection, it is worth mentioning that when heating rates are sufficiently slow (0.1 °C/min) the $L_\beta \rightarrow L_\alpha$ transition of dipalmitoylphosphatidylethanolamine can be resolved into at least two components which merge at higher scanning rates [24]. Moreover, it was reported by these workers that the $L_c \rightarrow L_\alpha$ transition of L-dipalmitoylphosphatidylethanolamine remains a single-component thermal transition even at a heating rate of 0.1 °C/min.

One possible interpretation of the molecular mechanism associated with the transition from L_β to L_α phase that can be made from the changes recorded at wide angles is that the disorder commences at the terminal methyl groups in the centre of the bilayer and proceeds along the chain towards the ester linkage with the glycerol. This process is followed by an increase in the area occupied by the molecule at the interface to a value characteristic of the L_α phase.

With regard to the conversion times of the $L_c \rightarrow L_\alpha$ and $L_\beta \leftrightarrow L_\alpha$ transitions measured in the temperature jump studies, it has been pointed out by Caffrey [11] that the values obtained in this manner reflect not only the intrinsic transit time but also the time required to supply or remove the heat associated with the transition. Nevertheless, the much slower $L_c \rightarrow L_\alpha$ conversion (about 10 s) as compared to the 2 s required for the $L_\beta \rightarrow L_\alpha$ transition in identical temperature jump experiments certainly reflects a significant difference in the intrinsic transit times. This difference is also seen in the case of transitions in dipalmitoylphosphatidylcholine. Thus, the overall transit time of the lamellar gel to liquid-crystal transition ($P_{\beta'} \rightarrow L_\alpha$) of dipalmitoylphosphatidylcholine is 2 s [8] while the transit time of the subtransition ($L_c \rightarrow L_\beta$) of this phospholipid, where a crystalline phase converts into a gel phase, is about 5 s [10]. It appears that, in general, the conversion of a crystalline phase into a higher-temperature phase is several times slower than the corresponding conversion of a lipid gel phase under identical heating conditions.

Acknowledgements

The work was aided by a grant from the Science and Engineering Research Council (U.K.) and by equipment purchased by the Central Research Fund of London University. B.G.T. was supported by the British Council.

References

1 Hitchcock, P.B., Mason, R., Thomas, K.M. and Shipley, G.G. (1974) Proc. Natl. Acad. Sci. USA 71, 3036–3040.
2 Harlos, K. and Eibl, H. (1980) Biochim. Biophys. Acta 601, 113–122.
3 Harlos, K. and Eibl, H. (1981) Biochemistry 20, 2888–2892.
4 Seddon, J.M., Cevc, G. and Marsh, D. (1983) Biochemistry 22, 1280–1289.
5 Seddon, J.M., Cevc, G., Kaye, R.D. and Marsh, D. (1984) Biochemistry 23, 2634–2644.
6 Mantsch, H.H., Hsi, S.C., Butler, K.W. and Cameron, D.G. (1983) Biochim. Biophys. Acta 728, 325–330.
7 Chang, H. and Epand, R.M. (1983) Biochim. Biophys. Acta 728, 319–324.
8 Caffrey, M. and Bilderback, D.H. (1984) Biophys. J. 45, 627–631.
9 Laggner, P. (1984) in Structural Biological Applications of X-ray Absorption, Scattering and Diffraction (Chance, B.

and Bartunik, H.D., eds.), pp. 171–182, Academic Press, London.
10 Tenchov, B.G., Lis, L.J. and Quinn, P.J. (1987) Biochim. Biophys. Acta 897, 143–151.
11 Caffrey, M. (1985) Biochemistry 24, 4826–4844.
12 Tamura-Lis, W., Lis, L.J. and Quinn, P.J. (1987) J. Phys. Chem. 91, 4625–4627.
13 Laggner, P., Lohner, K. and Müller, K. (1987) Mol. Cryst. Liq. Cryst. 151, 373–388.
14 Tenchov, B.G., Boyanov, A.I. and Koynova, R.D. (1984) Biochemistry 23, 3553–3558.
15 Boyanov, A.I., Koynova, R.D. and Tenchov, B.G. (1986) Chem. Phys. Lipids 39, 155–163.
16 Nave, C., Helliwell, J.R., Moore, P.R., Thompson, A.W., Worgan, J.S., Greenall, R.J., Miller, A., Burley, S.K., Bradshaw, J., Pigram, W.J., Fuller, W., Siddons, D.P., Deutsch, M. and Tregear, R.T. (1985) J. Appl. Cryst. 18, 396–403.
17 Helliwell, J.R., Greenough, T.J., Carr, P.D., Rule, S.A., Moore, P.R., Thomson, A.W. and Worgan, J.S. (1982) J. Phys. E15, 1363–1372.
18 Bunn, C.W. and Howells, E.R. (1954) Nature (London) 174, 549–551.
19 Seddon, J.M., Harlos, K. and Marsh, D. (1984) J. Biol. Chem. 258, 3850–3854.
20 Eliel, E.G. (1962) Stereochemistry of Carbon Compounds. Ch. IV, McGraw-Hill, New York.
21 Hauser, H., Pascher, L., Pearson, R.H. and Sundell, S. (1981) Biochim. Biophys. Acta 650, 21–51.
22 Hatta, I., Imaizumi, Sh. and Akutsu, Y. (1984) J. Phys. Soc. (Japan) 53, 882–888.
23 Hatta, I., Suzuki, K. and Imaizumi, Sh. (1983) J. Phys. Soc. (Japan) 53, 2790–2797.
24 Chowdhry, B.Z., Lipka, G. and Sturtevant, J.M. (1984) Biophys. J. 46, 419–422.
25 Sakurai, I., Sakurai, T., Seto, T. and Iwayanagi, S. (1983) Chem. Phys. Lipids 32, 1–11.